

**Contract No:**

This document was prepared in conjunction with work accomplished under Contract No. DE-AC09-08SR22470 with the U.S. Department of Energy (DOE) Office of Environmental Management (EM).

**Disclaimer:**

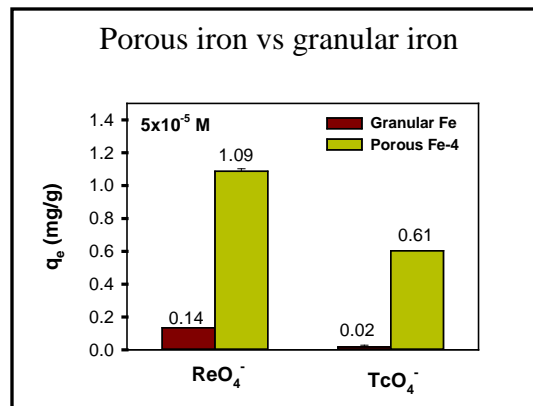
This work was prepared under an agreement with and funded by the U.S. Government. Neither the U. S. Government or its employees, nor any of its contractors, subcontractors or their employees, makes any express or implied:

- 1 ) warranty or assumes any legal liability for the accuracy, completeness, or for the use or results of such use of any information, product, or process disclosed; or
- 2 ) representation that such use or results of such use would not infringe privately owned rights; or
- 3) endorsement or recommendation of any specifically identified commercial product, process, or service.

Any views and opinions of authors expressed in this work do not necessarily state or reflect those of the United States Government, or its contractors, or subcontractors.

## Bimetallic Porous Iron (pFe) Materials for Remediation/Removal of Tc from Aqueous Systems

**Project highlight:** Remediation of Tc remains an unresolved challenge at Savannah River Site and other Department of Energy sites. In this project, we developed novel bimetallic porous iron materials for Tc removal from aqueous systems. Data showed that the porous iron is much more effective in removing  $\text{TcO}_4^-$  ( $\times 30$ ) and  $\text{ReO}_4^-$  ( $\times 8$ ) from artificial groundwater than granular iron. Tc K-edge X-ray absorption near-edge structure spectroscopy indicated that Tc speciation on the porous iron was 18% adsorbed  $\text{TcO}_4^-$ , 28% Tc(IV) in Tc dioxide and 54% Tc(IV) incorporated into the structure of Fe hydroxide. The Zn-deposited porous iron was outstanding among the six bimetallic porous iron materials, with a capacity increase of  $>100\%$  for  $\text{TcO}_4^-$  removal and of 50% for  $\text{ReO}_4^-$  removal, compared to the original porous iron. These results provide a highly applicable platform for solving critical Department of Energy and industrial needs related to nuclear environmental stewardship and nuclear power production.



## Awards and Recognition

N/A

## Intellectual Property Review

This report has been reviewed by SRNL Legal Counsel for intellectual property considerations and is approved to be publically published in its current form.

## SRNL Legal Signature

---

Signature

---

Date

## Bimetallic Porous Iron (pFe) Materials for Remediation/Removal of Tc from Aqueous Systems

Project Team: Dien Li (Primary), Simona Murph, Daniel I. Kaplan, Kathryn Taylor-Pashow, Miles Denham, and John Seaman (University of Georgia)

Subcontractor: University of Georgia

Thrust Area: Environmental Stewardship

Project Start Date: October 1, 2016

Project End Date: September 20, 2017

**Abstract:** Remediation of Tc remains an unresolved challenge at SRS and other DOE sites. The objective of this project was to develop novel bimetallic porous iron (pFe) materials for Tc removal from aqueous systems. We showed that the pFe is much more effective in removing  $\text{TcO}_4^-$  ( $\times 30$ ) and  $\text{ReO}_4^-$  ( $\times 8$ ) from artificial groundwater than granular iron. Tc K-edge XANES spectroscopy indicated that Tc speciation on the pFe was 18% adsorbed  $\text{TcO}_4^-$ , 28% Tc(IV) in Tc dioxide and 54% Tc(IV) into the structure of Fe hydroxide. A variety of catalytic metal nanoparticles (i.e., Ni, Cu, Zn, Ag, Sn and Pd) were successfully deposited on the pFe using scalable chemical reduction methods. The Zn-pFe was outstanding

among the six bimetallic pFe materials, with a capacity increase of  $>100\%$  for  $\text{TcO}_4^-$  removal and of  $50\%$  for  $\text{ReO}_4^-$  removal, compared to the pFe. These results provide a highly applicable platform for solving critical DOE and industrial needs related to nuclear environmental stewardship and nuclear power production.

### FY2017 Objectives

- Prepare and characterize new bimetallic materials comprised of porous iron (pFe) modified with catalytically active metallic nanoparticles (e.g., Ni, Cu, Zn, Ag, Sn and Pd)
- Evaluate the novel bimetallic pFe materials for Tc removal from a wide range of aqueous media representative of: 1) groundwater conditions (e.g., pH, Eh,  $\text{Fe}^{2+}$  and humic acid or organic ligands), and 2) extreme waste stream conditions (e.g., high pH, salt concentration,  $\text{NO}_3^-$ , and  $\text{CO}_3^{2-}$ )
- Characterize Tc binding chemistry with bimetallic pFe materials synchrotron radiation X-ray absorption fine structure (XAFS) to provide information about its chemical speciation and bonding environment
- Develop technologies to seal bound (adsorbed or reduced) Tc in the pore structures using easily injectable  $\text{Na}_2\text{SiO}_3$  or  $\text{MnSO}_4 + \text{KMnO}_4$

### Introduction

$^{99}\text{Tc}$  is a major long-life fission product during nuclear power generation. Over the years, Tc has been inadvertently introduced into the environment from leaks at waste storage facilities.  $^{99}\text{Tc}$  currently is one of the key risk drivers at the Savannah River Site (SRS) and other DOE environmental management sites (most notably the Hanford Site, Paducah Gaseous Diffusion Plant, and Oak Ridge National Laboratory). The most common chemical form of Tc in liquid nuclear wastes and in the environment is anionic pertechnetate ( $\text{TcO}_4^-$ ).  $\text{TcO}_4^-$  displays limited adsorption onto common sediment minerals and is highly mobile making it difficult to capture or to be immobilized.<sup>1</sup> As the stockpile of  $^{99}\text{Tc}$ -bearing nuclear waste continues to increase rapidly, novel sequestration technologies are needed to reduce its potential contamination of the environmental and living organisms.

With current technologies, quaternary amine-based resins have been used to remove Tc.<sup>2</sup> However, these resins are expensive and have only modest  $\text{TcO}_4^-$  loading capacities from the raffinate waste streams. Chemical reductants (e.g.,  $\text{Fe}_3\text{S}_4$ , soluble or structural  $\text{Fe(II)}$ )<sup>3</sup> and some bacteria<sup>4</sup> can reduce  $\text{Tc(VII)}$  to the sparingly soluble  $\text{Tc(IV)}$ . However, the resulting  $\text{Tc(IV)O}_2 \cdot 1.6\text{H}_2\text{O}$  has a solubility of  $1.5 \times 10^{-8}$  M in groundwater,<sup>5</sup> which greatly exceeds the EPA's maximum contaminant level of  $5 \times 10^{-10}$  M, and is readily re-oxidized and re-mobilized under most environmental conditions<sup>6</sup>. Tc reduction to form sulfides (e.g.,  $\text{Tc}_2\text{S}_7$ )<sup>7</sup> or embedding into other sulfide phases<sup>8</sup> or iron oxide waste forms<sup>9</sup> have also been investigated. However, these methods are not practical for many applications. There are currently no demonstrated technologies that are highly efficient and cost-effective for separation of Tc-containing nuclear waste streams and remediation of aqueous Tc in the contaminated sites.

In this project, we evaluated cost-effective porous iron for  $\text{TcO}_4^-$  and  $\text{ReO}_4^-$  sequestration from artificial groundwater, and investigated the Tc speciation and removal mechanisms on the porous iron. Further, we also developed chemical reduction methods that allowed us to deposit successfully catalytic metal nanoparticles, namely Ni, Cu, Zn, Ag, Sn and Pd, on the macro-pore structure of the porous iron material. The new bimetallic pFe materials were evaluated for the sequestration of  $\text{ReO}_4^-$  and  $\text{TcO}_4^-$  from artificial groundwater.

## Approach

The porous iron (pFe) samples were provided by our collaborator, North America Höganäs. The pFe samples were characterized by a number of analytical techniques to elucidate their morphology, size, composition, and porosity. Specifically, we used powder X-ray diffraction (XRD), scanning electron microscopy (SEM), energy dispersive X-ray spectroscopy (EDS) and BET surface area using Kr as the adsorption probe for its characterization.

pFe materials were used as template for creation of bimetallic catalytic materials with tailored and tunable structural, optical and surface properties. Six different metallic nanoparticles, namely Ni, Cu, Zn, Ag, Sn and Pd, were grown onto porous iron by straightforward wet chemical reduction methods that are amenable for scaling up. Basically, metal salts were reduced in water under ambient conditions, with a reducing agent to yield spherical nanoparticles onto the pFe substrates. By employing these experimental conditions, one could preserve the structural integrity of porous Fe, which is critical in this study. A variety of characterization techniques including SEM and EDS mapping were used to evaluate the physico-chemical properties of these materials.

The porous iron (pFe) and six bimetallic pFe (i.e., Ni-pFe, Cu-pFe, Zn-pFe, Ag-pFe, Su-pFe and Pd-pFe), in comparison with granular metallic iron purchased from Aldrich-Sigma, were evaluated for  $\text{TcO}_4^-$  and its surrogate ( $\text{ReO}_4^-$ ) from artificial groundwater under atmospheric ( $P_{\text{CO}_2} = 10^{-3.5}$  atm) conditions. Sorption coefficient ( $K_d$ , mL/g) and the equilibrium sorption capacity ( $q_e$ , mg/g) were calculated using formula 1 and 2, respectively:

$$K_d = \frac{C_0 - C_e}{C_e} \times \frac{V}{M} \quad (1)$$

$$q_e = \frac{(C_0 - C_e) \times V}{M} \quad (2)$$

where  $C_0$  and  $C_e$  were Tc or Re concentrations before and after adsorption, respectively,  $V$  was the total volume of liquid phase (i.e., groundwater), and  $M$  was the mass of the solid material.

Oxidation state and chemical bonding of Tc on the porous iron materials were investigated using synchrotron radiation X-ray absorption near-edge structure (XANES) and extended X-ray absorption fine structure (EXAFS). After batch experiments, Tc K-edge XANES and EXAFS spectra of the porous iron samples were collected using the Sector 20-BM beamline at the Advanced Photon Source (APS) (Argonne National Lab, Argonne, IL). The APS sector 20-BM beam line employed a Si(111) double crystal monochromator detuned 15% for harmonic rejection. The fluorescence detector had a four-layer Al foil filter to suppress the Fe fluorescence. The Tc K-edge XANES data were processed and fitted by linear combination fit (LCF) using the software Athena.

## Results/Discussion

### 1. Characterization of porous iron

The results show that the porous iron has a sponge-like porous structure (Fig. 1A) with a BET surface area of  $0.95 \text{ m}^2/\text{g}$ , pore volume of  $0.0068 \text{ mL/g}$ , and average pore diameter of  $364 \text{ \AA}$ . It is  $>92\%$  amorphous and  $\alpha$ -iron with small amounts of Fe and Al oxides (Figure 1B and 1C).

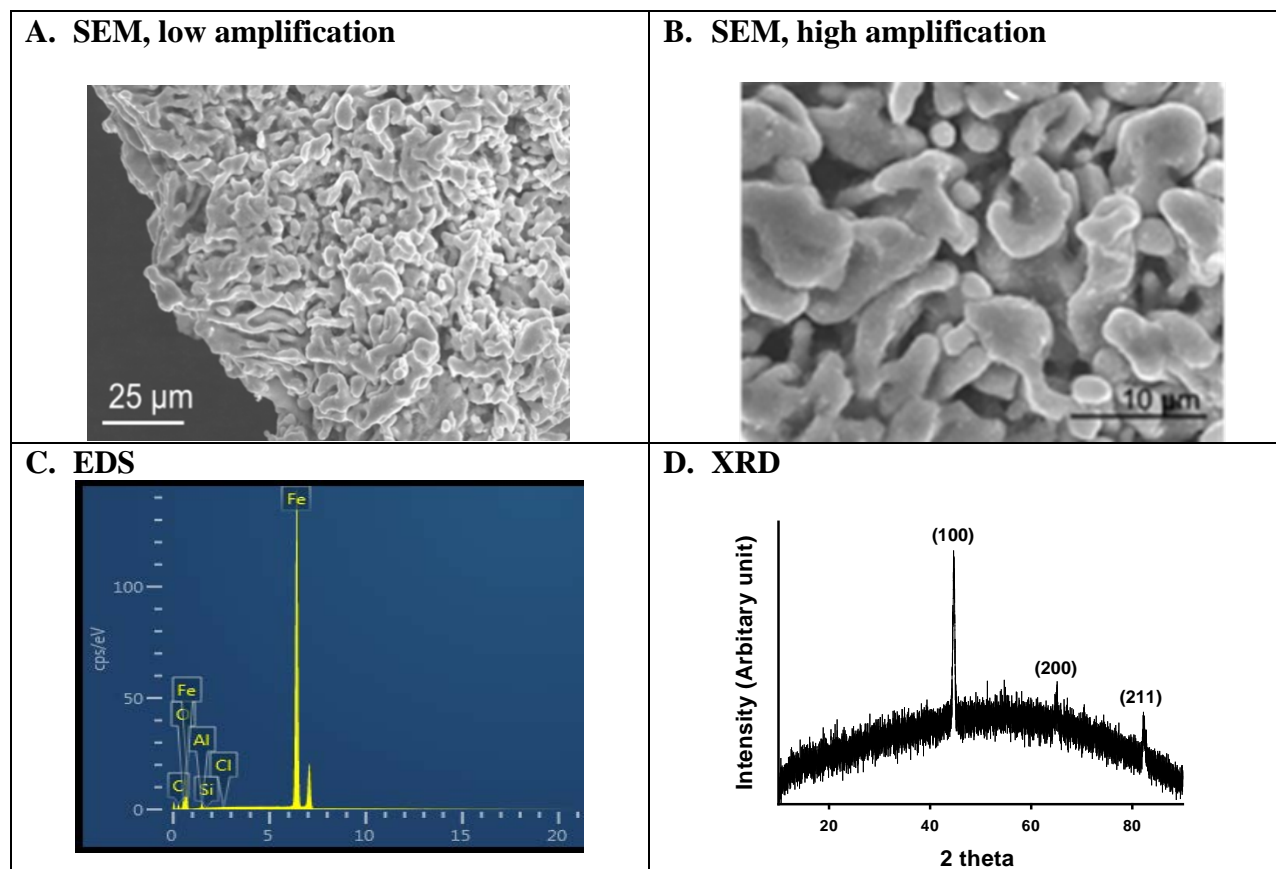


**Figure 1.** SEM images (A and B), EDS spectrum (B) and XRD pattern (C) of porous iron

### 2. Removal capacity of porous iron for $\text{TcO}_4^-$ and $\text{ReO}_4^-$ from artificial groundwater

The porous iron was much more effective than granular iron for both removal of both  $\text{TcO}_4^-$  and  $\text{ReO}_4^-$  from artificial groundwater. With the initial concentration of  $5 \times 10^{-5} \text{ M}$ , the removal

quantity of the porous iron was ~8 times greater for  $\text{ReO}_4^-$  and 30 times higher for  $\text{TcO}_4^-$  than the granular iron (Figure 2A). With the Tc concentration of  $3.2 \times 10^{-6}$  M present in artificial groundwater, the sorption coefficient of the granular iron was nearly zero for  $\text{TcO}_4^-$  removal, while the sorption coefficient of the porous iron was 2580 mL/g. Further, the removal capacity of the porous iron was demonstrated to be as high as 25 mg Tc per a gram of this material (Figure 2B).

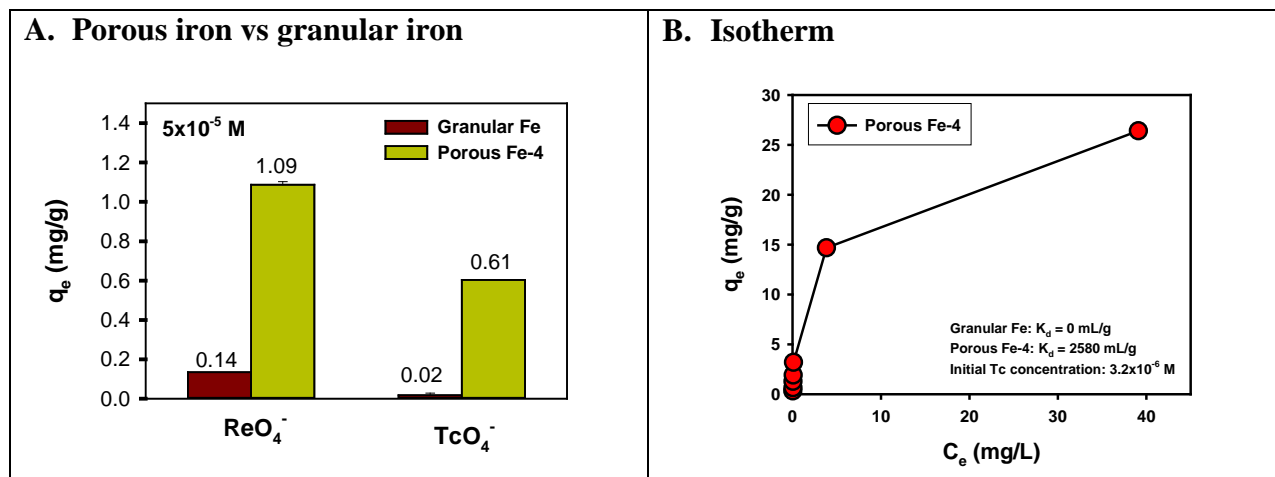


**Figure 2.** Removal capacity of porous iron for  $\text{TcO}_4^-$  and  $\text{ReO}_4^-$  from artificial groundwater. (A) Porous iron versus granular iron. (B) Isotherm of porous iron for  $\text{TcO}_4^-$  removal.

### 3. Tc speciation on the porous iron

Tc K-edge XANES spectra of two different porous iron samples are shown in Figure 3A. These spectra were compared with the spectra of ammonia pertechnetate, Tc(IV) dioxide and Tc(IV) co-precipitated goethite. The results show that both oxidation state species, namely  $\text{TcO}_4^-$  and reduced Tc(IV), on the porous iron samples after exposed to  $\text{TcO}_4^-$  in artificial groundwater. Linear combination fitting (LCF) indicated that, in the case of porous iron 1, there were 44.2% Tc(VII), 24.6% Tc(IV) in Tc dioxide and 31.2% Tc(IV) in goethite, while in the case of porous iron 4, there were 18.0% Tc(VII), 28.3% Tc(IV) in Tc dioxide and 53.7% Tc(IV) in goethite (Figure 3B).

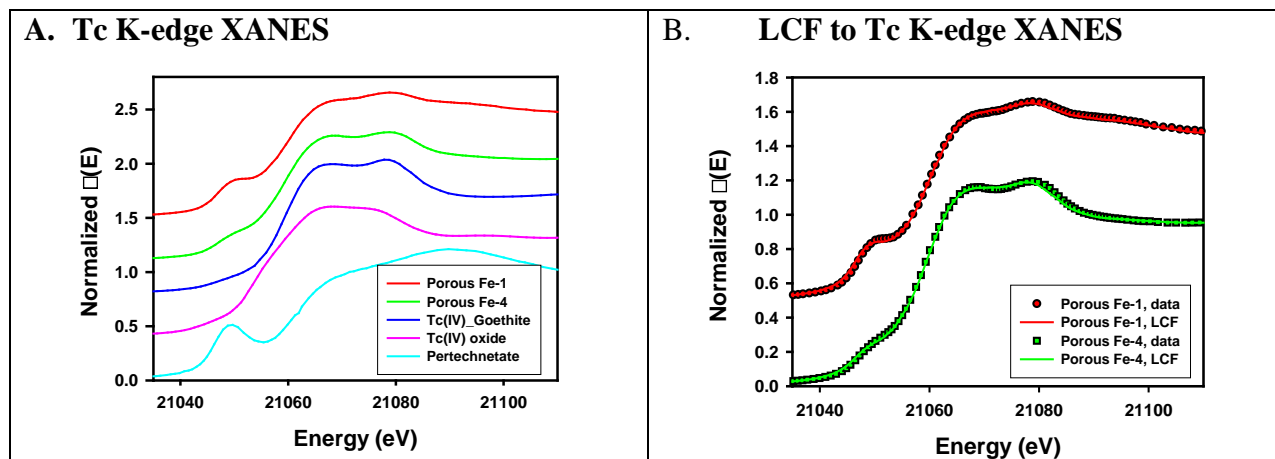




**Figure 3.** Tc K-edge XANES spectra of two different porous iron products in comparison with the spectra of model compounds (ammonia pertechnetate, Tc(IV) dioxide and Tc(IV) co-precipitated goethite) (A). The porous iron spectra were fitted through linear combination fitting (LCF) of the model compounds (B).

#### 4. Characterization of bimetallic porous iron

The six bimetallic pFe samples (i.e., Ni-pFe, Cu-pFe, Zn-pFe, Ag-pFe, Su-pFe and Pd-pFe) were characterized by using XRD, SEM, EDS and BET surface area and pore size measurement to elucidate their morphology, size, composition, and porosity. The SEM images and EDS data of representative Zn-pFe are shown in Figure 4. After deposition of the catalytic metal nanoparticles, the pore structure of the metal-deposited porous iron was preserved (Figure 4A). Metal nanoparticles of ~50 nm (estimated media particle size) were grown on the external and pore surfaces of porous iron (Figure 4B). Zn (and other metals as well) was detected in the EDS spectrum (Figure 4C) and Zn  $L_{\alpha_{1,2}}$  face scanning overlapped on the electron image (Figure 4D). The nanoparticle's loading varied for each individual metal, from 0.6 wt % to 2.0 wt %.

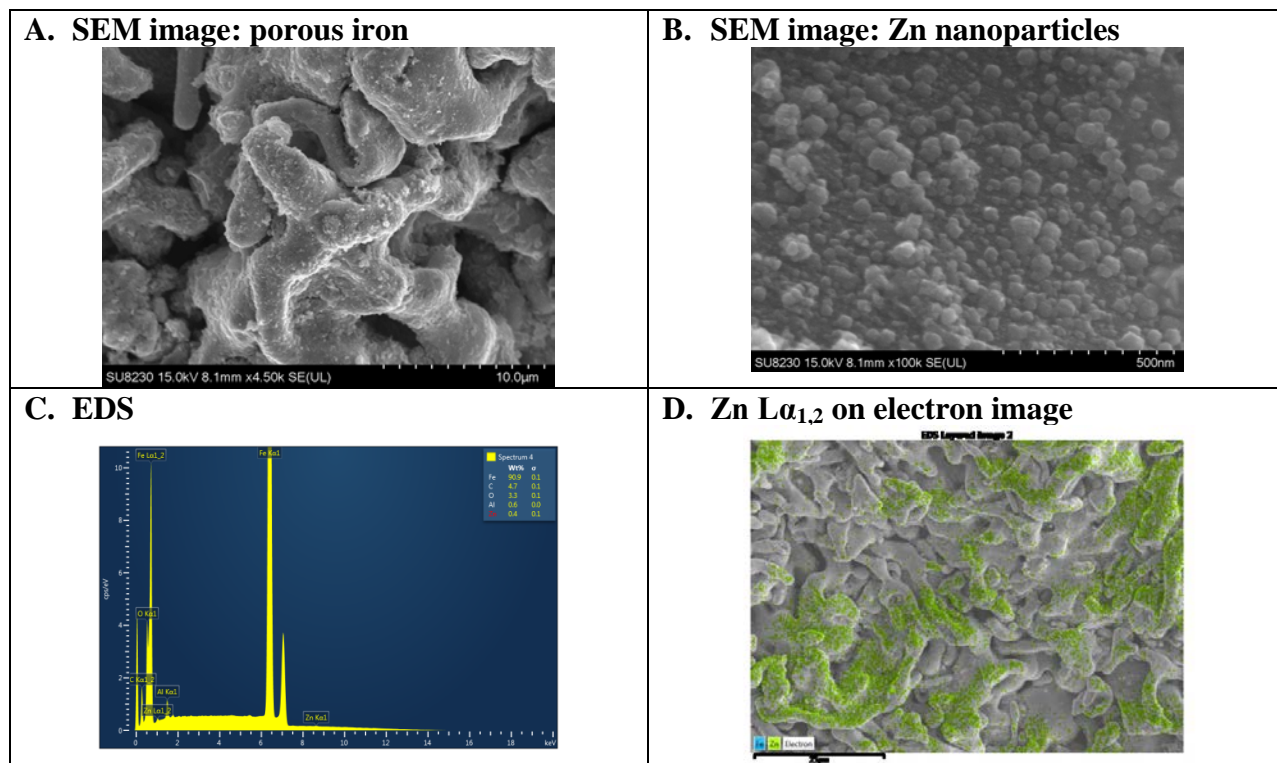


**Figure 4.** SEM images (A and B), EDS spectrum (C) and Zn  $L_{\alpha_{1,2}}$  on electron image (D) of the Zn-deposited porous iron

#### 5. Removal capacity of bimetallic porous iron for $\text{ReO}_4^-$ from artificial groundwater

The six metal-deposited porous iron materials were evaluated for  $\text{ReO}_4^-$  removal from artificial groundwater. Their sorption coefficient ( $K_d$ , mL/g) (A) and removal quantity (mg/g) (B), in comparison with granular and original porous iron, are shown in Figure 5. Zn-deposited porous iron was outstanding among the six metal-deposited porous iron materials for  $\text{ReO}_4^-$

removal. Data show that the Zn-pFe was more effective than original porous iron for  $\text{ReO}_4^-$  removal at three different initial concentrations of  $\text{ReO}_4^-$ . This trend was especially significant at the higher initial Re concentration. At the initial Re concentration of  $5 \times 10^{-3}$  M, the removal capacity of Zn-pFe increased by ~50% compared to the original porous iron.

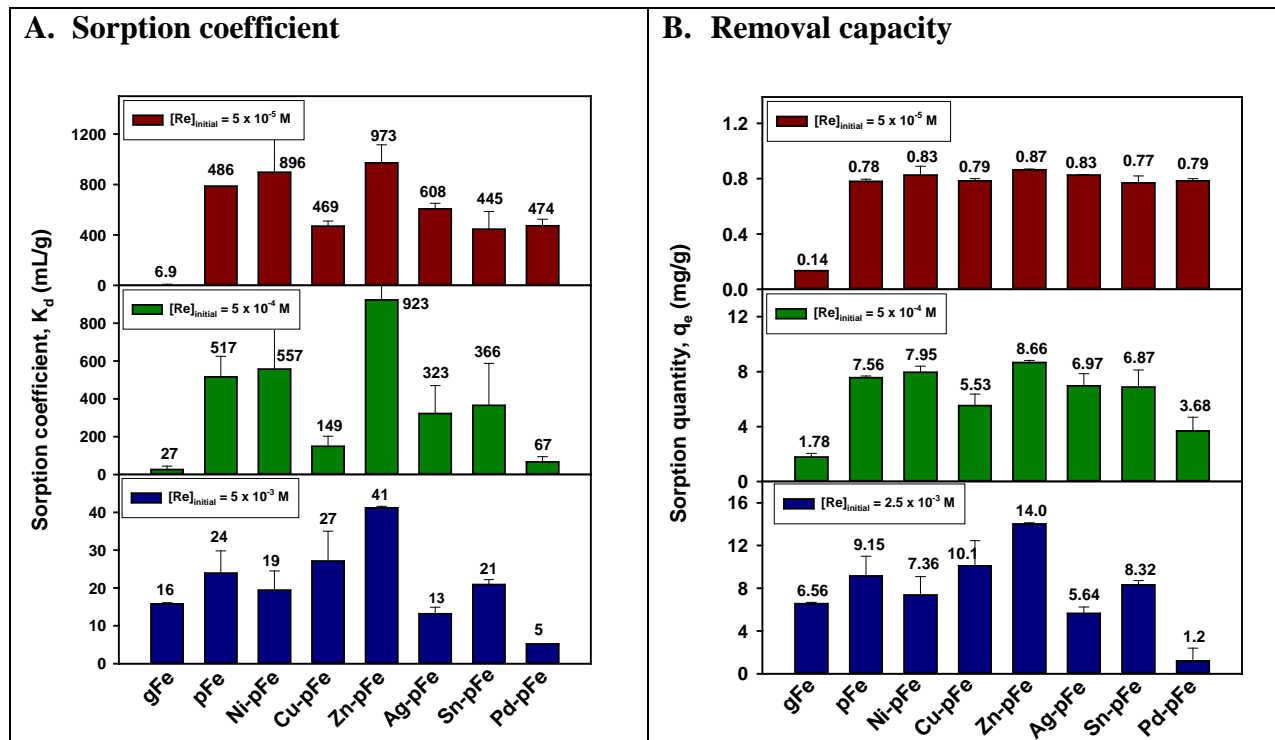


**Figure 5.** Sorption coefficient ( $K_d$ , mL/g) (A) and removal quantity (mg/g) (B) of six metal-deposited porous iron samples in comparison with granular and original porous iron for  $\text{ReO}_4^-$  removal from artificial groundwater (gFe = granular zero valent iron, pFe = porous iron, M-pFe = porous iron deposited with the catalytic metal nanoparticle M).

## 6. Removal capacity of bimetallic porous iron for $\text{TcO}_4^-$ from artificial groundwater

Similarly, the six metal-deposited porous iron materials were evaluated for  $\text{TcO}_4^-$  removal from artificial groundwater. Their sorption coefficient ( $K_d$ , mL/g) (A) and removal quantity (mg/g) (B), in comparison with granular and original porous iron samples, are shown in Figure 6. Once again, Zn-deposited porous iron was outstanding among the six metal-deposited porous iron materials for  $\text{TcO}_4^-$  removal. Zn-pFe was more effective than original porous iron for  $\text{TcO}_4^-$  removal. Specifically, at the initial Tc concentration of  $1.1 \times 10^{-3}$  M and solid / liquid ratio of 2 g/L, the removal capacity of Zn-pFe for  $\text{TcO}_4^-$  removal increased by >100% when compared to the original porous iron (Figure 6B).

A. Sorption coefficient	B. Removal capacity
-------------------------	---------------------



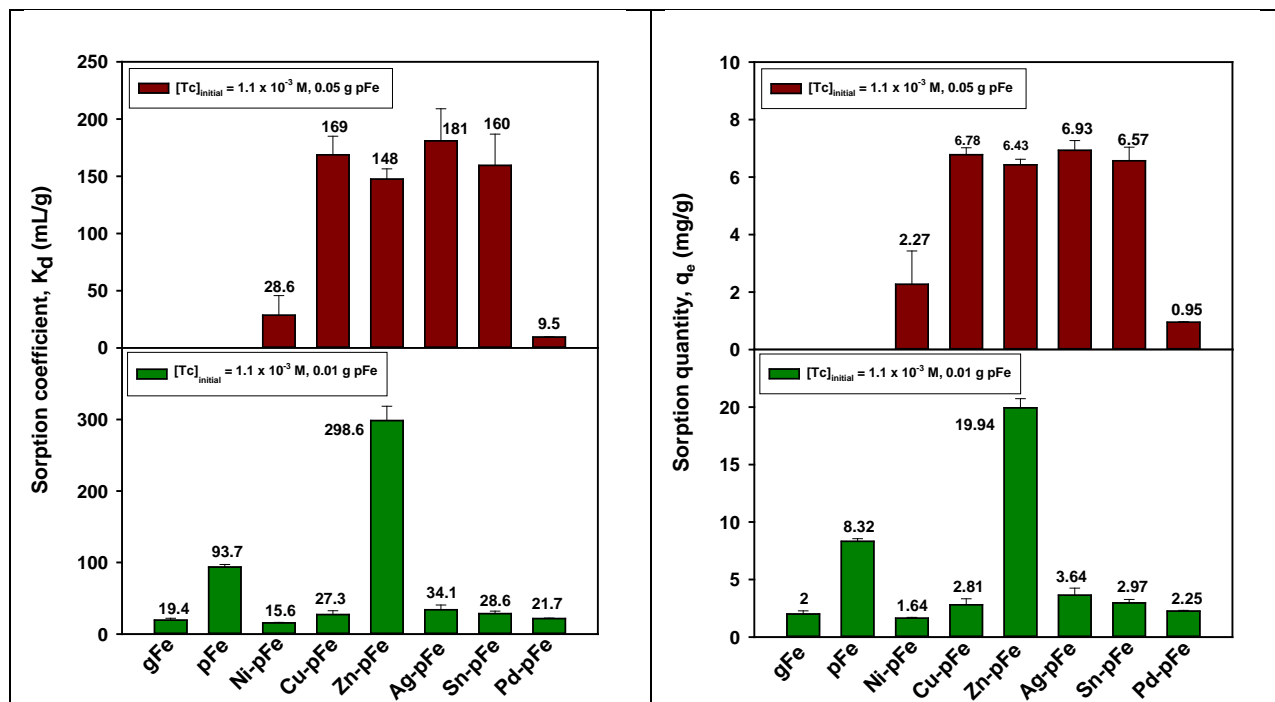


**Figure 6.** Sorption coefficient ( $K_d$ , mL/g) (A) and removal quantity (mg/g) (B) of the six metal-deposited porous iron samples in comparison with granular and original porous iron materials for  $TcO_4^-$  removal from artificial groundwater (gFe = granular zero valent iron, pFe = porous iron, M-pFe = porous iron deposited with the catalytic metal nanoparticle M).

### FY2017 Accomplishments

- Porous Fe is much more effective for removal of  $TcO_4^-$  and  $ReO_4^-$  from groundwater than granular zero valent iron. The capacity of the porous iron for  $TcO_4^-$  removal from groundwater can reach as high as 25 mg Tc/ g Fe
- Tc K-edge XAFS data indicated that Tc species on the porous iron were both reduced Tc(IV) and  $TcO_4^-$ . The percentage of the reduced Tc(IV) varied from 56% to 82%. Data show that the Tc(IV) is dominantly incorporated into the structure of Fe oxide / hydro-oxide, which are Fe corrosion products; and to lesser extent, to form Tc(IV) dioxide, which is quite beneficial as it will greatly decrease the re-oxidation and re-mobilization of Tc(IV)
- New chemical reduction methods were developed to deposit the second metal nanoparticles on porous iron and thus to make new bimetallic pFe
- Zn-pFe has been demonstrated to be outstanding among the six bimetallic pFe materials for  $TcO_4^-$  and  $ReO_4^-$  removal from groundwater. Compared to porous iron, the capacity of the Zn-pFe increased by ~50% for  $ReO_4^-$  and by >100% for  $TcO_4^-$  removal from artificial groundwater

### Future Directions

- Proposals to DOE EM Soil & Groundwater Remediation Program, International Program, and DOE Nuclear Energy program
- Submit a manuscript describing these results to the American Chemical Society journal, *Environmental Science and Technology*

- Evaluate porous iron and Zn-pFe for  $\text{TcO}_4^-$  removal under different environmental and geochemical conditions (i.e., pH, Eh, solution chemistry) and for  $\text{TcO}_4^-$  separation from liquid nuclear wastes
- Field demonstration of cost-effective porous iron for Tc attenuation at SRS and other DOE contaminated sites

## FY 2017 Publications/Presentations

1. **Dien Li**, Simona E. Murph, Kaitlin Coopersmith, Daniel I. Kaplan, Kathryn Taylor-Pashow, John C. Seaman, H. Chang, M. Tandukar, Pertechetate immobilization from aqueous Media by bimetallic porous iron composites, Migration 2017, Barcelona, Spain, September 10-15, **2017**.
2. John C. Seaman, **Dien. Li**, E. Dorward, J. Cochran, H.S. Chang, M. Tandukar, F.M Coutelot, and D. Kaplan, Immobilization of radioactive materials using porous iron composite media, Waste Management 2018, Phoenix.
3. **Dien Li**, Shani Egodawatte, Daniel I. Kaplan, Sarah C. Larsen, Steven M. Serkiz, John C. Seaman, Kirk G. Scheckel, Jinru Lin, Yuanming Pan, Extraction of Uranium from Seawater Simulant by Functionalized Magnetic Mesoporous Silica Nanoparticles: Capacity and Molecular Mechanisms, Submitted to *Environ. Sci. Technol.* 2017.
4. **Dien Li**, Daniel I. Kaplan, John C. Seaman, Brian A. Powell, Allison Sams, Steve M. Heald, Chengjun Sun, Sequestration of pertechnetate ( $\text{TcO}_4^-$ ), iodide ( $\text{I}^-$ ) and iodate ( $\text{IO}_3^-$ ) from groundwater by cost-effective organoclays and granular activated carbon: Capacity and chemical speciation, To be submitted to *J. Hazard. Mater.*, **2017**.
5. **Dien Li**, Daniel I. Kaplan, John C. Seaman, Brian Powell, Allison Sams, Steve M. Heald, and Chengjun Sun, Effective Removal of Pertechnetate ( $\text{TcO}_4^-$ ), Iodide ( $\text{I}^-$ ) and Iodate ( $\text{IO}_3^-$ ) from Groundwater by Organoclays and Granular Activated Carbon, 2017 AIChE Annual Meeting, Minneapolis, Oct 29-Nov 3, 2017.

## References

1. Icenhower, J. P.; Qafoku, N. P.; Zachara, J. M.; Martin, W. J., The biogeochemistry of technetium: A review of the behavior of an artificial element in the natural environment. *American Journal of Science* **2010**, 310, (8), 721-752.
2. Liang, L. Y.; Gu, B. H.; Yin, X. P., Removal of technetium-99 from contaminated groundwater with sorbents and reductive materials. *Separations Technology* **1996**, 6, (2), 111-122.
3. Peretyazhko, T.; Zachara, J. M.; Heald, S. M.; Jeon, B. H.; Kukkadapu, R. K.; Liu, C.; Moore, D.; Resch, C. T., Heterogeneous reduction of Tc(VII) by Fe(II) at the solid-water interface. *Geochimica Et Cosmochimica Acta* **2008**, 72, (6), 1521-1539.
4. Plymale, A. E.; Fredrickson, J. K.; Zachara, J. M.; Dohnalkova, A. C.; Heald, S. M.; Moore, D. A.; Kennedy, D. W.; Marshall, M. J.; Wang, C. M.; Resch, C. T.; Nachimuthu, P., Competitive reduction of pertechnetate ( $\text{TcO}_4^-$ ) by dissimilatory metal reducing bacteria and biogenic Fe(II). *Environmental Science & Technology* **2011**, 45, (3), 951-957.

5. Li, D.; Kaplan, D. I., *Solubility of Technetium Dioxides ( $TcO_2$ -c,  $TcO_2 \cdot 1.6H_2O$  and  $TcO_2 \cdot 2H_2O$ ) in Reducing Cementitious Material Leachates: A Thermodynamic Calculation*. Savannah River National Laboratory: Aiken, SC 20908, 2013.
6. Fredrickson, J. K.; Zachara, J. M.; Plymale, A. E.; Heald, S. M.; McKinley, J. P.; Kennedy, D. W.; Liu, C. X.; Nachimuthu, P., Oxidative dissolution potential of biogenic and abiogenic  $TcO_2$  in subsurface sediments. *Geochimica Et Cosmochimica Acta* **2009**, 73, (8), 2299-2313.
7. Liu, Y.; Terry, J.; Jurisson, S., Pertechetate immobilization in aqueous media with hydrogen sulfide under anaerobic and aerobic environments. *Radiochimica Acta* **2007**, 95, (12), 717-725.
8. Fan, D. M.; Anitori, R. P.; Tebo, B. M.; Tratnyek, P. G.; Pacheco, J. S. L.; Kukkadapu, R. K.; Engelhard, M. H.; Bowden, M. E.; Kovarik, L.; Arey, B. W., Reductive Sequestration of pertechetate ( $TcO_4^-$ ) by nano zerovalent iron (nZVI) transformed by abiotic sulfide. *Environmental Science & Technology* **2013**, 47, (10), 5302-5310.
9. Um, W.; Chang, H. S.; Icenhower, J. P.; Lukens, W. W.; Serne, R. J.; Qafoku, N. P.; Westsik, J. H.; Buck, E. C.; Smith, S. C., Immobilization of 99-technetium (VII) by Fe(II)-goethite and limited reoxidation. *Environmental Science & Technology* **2011**, 45, (11), 4904-4913.

## Acronyms

APS	Advanced Photon Source
BET	Brunauer–Emmett–Teller
DOE	Department of Energy
EDS	Energy dispersive X-ray spectroscopy
EXAFS	Extended X-ray absorption fine structure
gFe	Granular zero valent iron
LCF	Linear combination fit
pFe	Porous iron
SEM	Scanning electron microscopy
SRS	Savannah River Site
XAFS	X-ray absorption fine structure
XANES	X-ray absorption near-edge structure
XRD	X-ray diffraction

## Intellectual Property

N/A

## Total Number of Post-Doctoral Researchers

0.5 of post-doctoral researcher involved through the subcontractor